

Last 10000 years variation in the intensity of OMZ-Core reconstructed from sediment of the Eastern Arabian Sea

Joshi, G.P.¹; Naik, S.S.¹; Banakar, V.K.²

1. CSIR-National Institute of Oceanography, Dona Paula, 403 004, Goa, India
Academy of Scientific and Innovative Research (AcSIR), Ghaziabad, 201002, India
2. Zeib Castle, La Oceana, behind International Centre, Dona Paula, 403 004, Goa, India

Abstract

The Arabian Sea Oxygen Minimum Zone (OMZ) is one of the most intense of the world ocean OMZs witnessing denitrification, hence, has implications to global climate. In order to understand the Holocene variations in the OMZ of this region, we retrieved a sediment core (BP3-GCR3) from a water depth of 500 m, which is presently swept by nearly anoxic waters of the core of the OMZ. The sedimentary oxide-bound Mn, a reliable redox proxy, exhibits a gradual decrease from ~14 ppm during the Early-Holocene to ~8 ppm during the Late-Holocene, suggesting a relatively less intense OMZ during the former period. The concentration of a suite of other redox-sensitive elements (Fe, Co and Ce) associated with the dispersed sedimentary oxide particulates also show a gradual and coherent decrease through the Holocene suggesting reduction of dissolved oxygen (DO) in the core of the OMZ towards the modern times. This intensification of OMZ seems to be a result of increased export production coupled with decreasing ventilation of thermocline waters through the Holocene. A one-time shift is observed at ~5.5 ka BP in the organic carbon content (OC) from ~2 % to ~10 % in core-top. This shift in OC content is also marked by rapid decrease of CaCO₃ by ~20 %, suggesting enhanced carbonate dissolution due to increased anoxia in the ambient waters caused by increased export production in the late Holocene.

Keywords: Eastern Arabian Sea, Sediment, Holocene, Palaeo-OMZ, Redox-sensitive elements.

1. Introduction

The Arabian Sea has a pronounced Oxygen Minimum Zone (OMZ) between 150 and 1200 m water depths (Wyrтки 1973), which is sustained due to upwelling-induced high productivity during the southwest monsoon and a poorly ventilated thermocline (Olson et al., 1993). The ventilation of the Arabian Sea OMZ is driven by the following water masses, viz., high salinity Persian Gulf Water (PGW: DO = $\sim 152 \mu \text{ mol kg}^{-1}$ or 2.5 ml l^{-1}) at $\sim 300 \text{ m}$ depth and the Red Sea Water (RSW: DO = $\sim 109 \mu \text{ mol kg}^{-1}$ or 3.5 ml l^{-1}) at $\sim 800 \text{ m}$ (Wyrтки, 1973; You, 1997). The primary source of highly oxygenated waters to the Arabian Sea is the intermediate water formed along the northern edge of the Antarctic Circumpolar Current (ACC) (McCreary et al., 2013). Factors controlling the oxygen balance in the Arabian Sea OMZ are however not uniform across the basin. The Arabian Sea OMZ is shifted eastward from the region of highest productivity (Naqvi et al., 1991; Morrison et al., 1999) primarily due to the enhanced advection of oxygenated waters and vertical eddy mixing in the western Arabian Sea (McCreary et al., 2013). Whereas, along the eastern coast of the Arabian Sea, the southern oxygenated waters advected by the Indian coastal undercurrent during summer and northern low-oxygen waters during winter balance the biological consumption of oxygen below this high productive region and are responsible in maintaining the OMZ (Resplandy et al., 2012). The modern OMZ with DO of $<0.1 \text{ ml l}^{-1}$ has been delineated utilizing measured DO and dissolved-Mn in the water column where both exhibit distinctly contrasting depth profiles (Saager et al., 1989) (Fig. 1).

The sediments deposited under an OMZ-environment differ in their geochemical characteristics from sediments deposited under an oxic environment, as many elements change their lower oxidation states (dissolved state) in OMZ (Saager 1994). For example, sedimentary Mn- and Fe- particulates preserve signatures of DO levels during their redox-transitions, whether precipitated and deposited or *vice-versa*. Under suboxic to anoxic conditions, sedimentary Mn-oxide undergoes reductive dissolution, releasing the Mn to the overlying water column and thus enriching the dissolved Mn-pool (Martin and Knauer 1984; Lewis and Luther 2000; Schenau et al., 2002). In the presence of highly oxic bottom waters, Mn migrates to oxygenated regions by advective and diffusive processes to ultimately precipitate as solid phase Mn (Mn-oxide and -hydroxides or -Mn-carbonates) (Grill 1982; Dickens and Owen 1994; Calvert and Pedersen 1996). This redox-dynamics of Mn is the primary cause for globally observed mirror-image type vertical distribution patterns of DO and dissolved Mn in marine regimes.

Several depth profiles of DO and dissolved Mn (dMn) across the OMZ in the Arabian Sea indicate that the oxidation/reduction boundary for Mn is at $\sim 40 \mu \text{ mol}$ of DO ($\sim 1 \text{ ml/L}$) (Lewis and

Luther 2000), i.e, within the suboxic environment. Fe oxidation occurs when DO is $>50 \mu\text{mol/l}$ (Tamura et al., 1976) suggesting that the redox boundaries of both the elements are close and hence behave nearly similar under similar redox conditions. Thus, the relative variations in oxide-Mn and Fe content in sediment swept by intense OMZ waters can be utilized to understand past fluctuations of the OMZ intensity at its core.

Cerium (Ce) and cobalt (Co) are also redox sensitive elements and are expected to behave in a same way as Mn and Fe during their removal to sediments. Under suboxic or anoxic conditions Ce^{4+} is reduced to Ce^{3+} and Co^{3+} to Co^{2+} and become components of the dissolved pool. These two elements are removed to sediment either as scavenged cations on the surface of particulate Mn-Fe oxides (German and Elderfield 1990; Pattan et al., 2005) or independently precipitate as oxide phases similar to Mn and Fe (see Rajani et al., 2005; Banakar et al., 2007). Therefore, both Ce and Co, like Mn and Fe can be used as proxy indicators for reconstructing changes in past OMZ (Frank et al., 1999; Pattan et al., 2005).

Past OMZ variations in the Arabian Sea have been shown to have direct links to regional monsoons and global climate (Reichart et al., 1998; Gupta et al., 2004; Lachkar et al., 2016), calcite dissolution (Naik et al., 2014) and variations in aragonite compensation depth (Singh 2007; Naidu et al., 2014). Hence, several previous studies were aimed at reconstructing the past OMZ variations using redox sensitive elements in sediments (Dickens and Owen, 1994; Schenau et al., 2002; Agnihotri et al., 2002; Weijden et al., 2006; Naik et al., 2014; Pattan et al., 2017), pteropod preservation (Singh et al., 2006; Singh, 2007), coccolithophores (Cabarcos et al., 2014), planktic foraminiferal assemblage and abundance (Singh et al., 2006, 2011, 2018), abundance and diversity of benthic foraminifera (Singh et al., 2015; Das et al., 2017; Verma et al., 2018) and biogeochemical modelling (Gaye et al., 2018). The temporal variations of denitrification via $\delta^{15}\text{N}$ preserved in sedimentary organic matter have also been used to understand past changes in the intensity of Arabian Sea OMZ (Altabet et al., 1995; Banakar et al., 2005; Singh et al., 2011; Kessarkar et al., 2018). The Al-normalized bulk composition of redox- elements has also been used to infer the redox-status of bottom waters (Agnihotri et al., 2003). Based on Al-normalized contents of redox-sensitive elements in a sediment core from the Eastern Arabian Sea (EAS) Agnihotri et al. (2003) demonstrated that the bottom-waters at ~ 600 m water depth remained mostly reducing throughout the Holocene. The lower Mn/Al in EAS sediments ($\sim 48 \pm 8$) (Agnihotri et al. 2003) compared to average shale (~ 106 ; Turekian and Wedepohl 1961) has been suggested to indicate that the sedimentary-Mn is mobilized out of sediment reservoir due to reducing environments (Somayajulu et al., 1994; Agnihotri et al., 2003; Sruthi et al., 2014; Pattan et al., 2017).

Although, the bulk-Mn composition has been used to reconstruct past OMZ variation in the Arabian Sea, a targeted investigation of redox-specific oxide-bound sedimentary Mn particulates is lacking. An overwhelming amount of bulk-Mn and Fe in sediment have their source in detrital silicates as indicated by average crustal composition (see Taylor and McLennan 1985). Therefore, a small variation in particulate Mn- or Fe content caused by redox-transition due to DO fluctuations in bottom waters may get subdued by the Mn and Fe associated with detrital silicates. This would therefore warrant extraction of redox-sensitive elements associated exclusively with dispersed oxide particulates. In the present study we report time-series of oxide bound Mn and Fe in a sediment core from the EAS along with other redox-sensitive trace elements (Co and Ce) to discuss the changes in the intensity of OMZ-core through the Holocene and its effects on organic- and inorganic- carbon burial.

2. Material and methods

A 5.3 m long sediment core (BP3-GCR3) from a water-depth corresponding to the core of modern OMZ (water depth of 500 m) was retrieved from the continental slope off Goa at 15° 35' N latitude and 72° 44' E longitude (Fig. 1) on board I.B. Boris Petrov Cruise No. 3, 2005. The modern vertical distribution of DO and dissolved – Mn (hereafter dMn) near the present sediment core location are shown as inset in Fig. 1. The age model for the top 1.3 m section of this sediment core is based on three AMS ¹⁴C dates. Nearly 1000 tests of mixed planktic foraminifera species were handpicked under microscope from coarse fractions and sent for AMS radiocarbon measurements to the University of Arizona. The measured radiocarbon ages were corrected for reservoir age of 622 y for EAS (Southon et al. 2002) and converted to calibrated calendar ages using CALIB 7.1 Radiocarbon Calibration Program (Stuiver and Reimer, 1993) with 1950 AD as the reference year (Table 1).

Finely ground, oven-dried, accurately weighed aliquots were subjected to extraction of dispersed authigenic oxide particulates in the sediment by using pH adjusted hydroxylamine hydrochloride leaching method (Rutberg et al., 2000; Bayon et al., 2002). The dried leachate (hydrolysate fraction) was dissolved in ultrapure 0.05M HNO₃ and analyzed on an in-house PerkinElmer Optima 7300 DV ICP-OES. Three manganese nodule standards from Japan (JMn-1) and USGS (A1 and P1) were also leached and analysed along with sample solutions to monitor the elemental recovery during extraction process. The analyzed results of Mn and Fe in reference standards, show >95% of recovery (Table 2). The 1 σ standard deviation based on eight measurements is ± 0.9 %.

The inorganic carbon (IC) content was measured using an in-house CM5130 Coulometer. The precision of the IC measurement is $\pm 0.8\%$ ($n = 15$) as obtained for an in-house standard (AAS 9-11). The IC content was converted to $\text{CaCO}_3\%$ by multiplying with a factor of 8.333. The organic carbon (OC) content was measured on an in-house Thermo Flash-1112 elemental analyser using finely ground and dried residue of the sediment after decarbonation using diluted HCl. The precisions of the OC measurement $\pm 1.5\%$ (1σ ; $n=21$) using sucrose as a standard.

3. Results

The oxide-bound Mn and Fe in the present sediment core vary from 6 ppm to 15 ppm, and 154 ppm to 682 ppm respectively with a mean of 11.5 ppm and 420 ppm respectively (Fig. 2a). Variation in oxide bound-Ce and Co content ranges from 0.3 ppm to 1.3 ppm and 0.3 to 0.9 ppm with a mean of 0.7 ppm and 0.6 ppm respectively (Fig. 2b). The variation in CaCO_3 ranges between 27 % and 53 %. Generally high CaCO_3 (~50 %) is evident during the Early Holocene, followed by a rapid reduction through Mid Holocene reaching lowest contents of ~30 % in the Late Holocene (Fig. 2d). The OC content varies from 1.5 % to 10.2 %, with distinctly low values during the Early Holocene (~1.7 %) with rapid increase to a maximum of 10.2 % in the core-top resulting in a Late Holocene mean of ~ 6.6 % (Fig. 2d). An increase in rate of sedimentation by a factor of 1.5 is recorded through the Holocene with around 10.5 cm/ky during the Early Holocene to around 15 cm/ky during Late Holocene (Fig. 3).

4. Discussion

The oxide-bound Mn and Fe concentrations in sediment reflect the extent of oxygenation at sediment-water interface resulting from changes in DO of the bottom water. The high content of particulate-Mn and Fe is characteristic of strongly oxidizing conditions. This is evident from the widespread occurrences of ferromanganese nodules in deep-sea basins where highly oxygenated deep and bottom waters prevail (see Banakar, 2010 and references therein).

A gradual decrease in both the oxide-bound elements from beginning of the Holocene towards present day (Fig. 2a) suggests an intensifying core of the OMZ through the Holocene. Prior to ~5.5 ka, the oxide-Mn and -Fe were generally higher than the average of 11.5 ppm and 420 ppm respectively, whereas, they were lower than their respective averages after 5.5 ka. When compared to the observed Mn oxidation/reduction boundary in the Arabian Sea OMZ (~40 μM DO) (Lewis and Luther 2000), the $<5\ \mu\text{M}$ DO in the modern OMZ core indicates that the Arabian Sea OMZ has been intensifying consistently through the Holocene. If we assume that the core-top (149 ± 118 y B.P; Table 1) oxide-Mn of 6 ppm represents DO within the modern core of the Arabian Sea OMZ, then higher oxide-Mn (> 6 ppm) throughout the preceding period suggests that the DO in the core of

OMZ has remained always higher than the present, which has led to decreased removal of sedimentary oxide-Mn to the surrounding water. This explanation is also applicable to the oxide-Fe as its variation is similar to oxide-Mn (Fig. 2a) and, in phase diagrams the redox boundary of Mn and Fe is at a similar Eh of ~ 0.2 V (at pH = 8 and bottom water temperatures of ~ 2 °C) (Glasby et al. 2010). The average content of Co and Ce are 0.6 ppm and 0.7 ppm respectively (Fig. 2b). These two elements are normally removed to (from) the sediment by precipitation (dissolution) of Mn-Fe oxide particulates as they are either readily scavenged by colloidal Fe-Mn oxide particulates or independently oxidize in the marine environment (Rajani et al., 2005; Banakar et al. 2007). The time-series of these two minor elements also are nearly similar to the Mn and Fe time-series, where they show similar gradual decrease from above average to below average at ~ 5.5 ka BP which suggest a shift of OMZ towards a more intense state (Fig. 2b).

The Arabian Sea is characterized by monsoon-induced high biological productivity (Banse, 1968; Qasim, 1977). Our study region lies under a low-salinity plume resulting from the Sahyadri (Western Ghats) runoff during the summer monsoon (Singh et al., 2006; Naik et al., 2015) and consequent stratified surface waters (Joseph and Freeland, 2005). This region experiences weak upwelling during summer whereas during winter, the cool and dry monsoon winds lead to evaporation, surface cooling and convection (Madhupratap et al., 1996; Kumar et al., 2000). Thus primary production is enhanced during both the seasons, but is comparatively higher during the summer monsoon (Bhattathiri et al., 1996). As the entire Holocene has witnessed mostly denitrifying and Mn-reducing conditions in the core of the OMZ, the sedimentary organic carbon (OC) deposited at depth swept by water of the OMZ-core should be a faithful indicator of export production at the present study location. Thus, the OC content in the present sediment core could be an indicator of monsoon driven productivity changes in the EAS, assuming absence of its dilution by terrigenous silicate matter. This assumption appears to be valid as the sedimentation rate changes by a factor of only 1.5 *vis-a-vis* a change in OC content by a factor of 7 (Fig. 3). The rapid increase of OC from ~ 2 % to 10 % (Fig. 2d) also occurs across ~ 5.5 ka in line with the decrease of Mn, Fe, Co and Ce from above the Holocene mean to below the mean at ~ 5.5 ka BP. These observations together indicate significantly enhanced productivity in the Arabian Sea, mid-Holocene onwards, probably as a result of intensified monsoon. The mid-Holocene reorganisation of monsoon speculated here is also evident in several previous reconstructions based on north Indian lake records (Prasad et al. 2014; Raj et al. 2015) and Indus discharge record (Staubwasser et al. 2003). This mid-Holocene monsoon reorganisation has been suggested important for understanding the rise and fall of Harappan urbanisation that was at its peak around 5 ka BP (Raikes 1964; Lawler 2008).

The CaCO₃ content from our study also exhibits a dramatic shift at ~5.5 ka from higher (~55 %) to lower (~35%) values (Fig. 2d) in contrast to the corresponding OC shift. The accumulation of CaCO₃ in sediments is mainly governed by surface productivity, rate of dissolution, and dilution by terrigenous material. Studies from the EAS show a Holocene CaCO₃ decrease as a result of carbonate dissolution (Bhushan et al. 2001; Naik et al. 2014; Nagoji and Tiwari 2017) or dilution by terrigenous silicates (Narayana et al. 2009). The increased sedimentation rate in the late Holocene by a factor of 1.5 seems to be insufficient to cause CaCO₃ reduction by a factor of 2. The drastic reduction of CaCO₃ after ~5.5 ka BP might therefore have been caused by dissolution resulting from a large increase in the OC supply to the seafloor (Naik et al. 2014). Increasing productivity causing increasing CaCO₃ dissolution can be seen in their mutually strong inverse relationship ($r = -0.8$) only when the OC content is $> 2\%$. This relationship reverses to a strong positive trend ($r = 0.9$) when the OC content is $< 2\%$ (Fig. 4). Thus, for the Arabian Sea sediments, the OC content of 2% appears to be critical for carbonate preservation.

The variation in OMZ intensity observed from Core BP3-GCR3 is in line with that of Core SK-17 (15°15'N; 72°58'E; water depth: 840 m) located in proximity (Fig. 1). Records of high-O₂ benthic assemblage from SK-17 show a gradual change from relatively oligotrophic, oxygen-rich bottom environment in the early Holocene to more eutrophic, oxygen-poor environment in the middle-late Holocene (Fig. 2c; Singh et al., 2015) which has been attributed to strengthening of the OMZ. Our observations are also supported by other studies in the vicinity, which show a gradual intensification of OMZ through the Holocene (Godad et al. 2017; Kessarkar et al. 2018). The oxygen depleted waters result from high rate of oxygen consumption in the water column due to high rates of organic matter generated from monsoon-driven productivity, combined with slow renewal of thermocline waters. The OC variations in core SK-17 which Singh et al., (2006) attribute to productivity changes show a trend similar to our results. Recent studies have shown that the Holocene productivity was lower in comparison to the last glacial maximum (LGM) and that the productivity increased during the late Holocene (Singh et al., 2011, Cabarcos et al., 2014, Singh et al., 2018). We carried out a comparison of our OC record to the *Globigerina bulloides*/*Globigerinoides ruber* ratios from SK-17 which was used as a productivity indicator (Fig. 2e; Singh et al., 2011). The low productivity during early to mid-Holocene has been suggested to be due an increase in the stratification of the upper ocean water column (Cabarcos et al., 2014) while the increase of productivity during the late Holocene was probably due to a moderate increase in winter monsoon wind-induced vertical mixing and/or sporadic upwelling (Cabarcos et al., 2014, Singh et

al., 2018). Our OC record increases from ~ 5.5 ka BP onwards and shows a sharp increase from ~2.5 ka BP, which compares well with the ratios from SK-17 indicating enhanced productivity.

We further compared the CaCO₃ content from BP3-GCR3 to the aragonite content from Core SK-17 (Fig. 2e). The aragonite content in sediments can be an indicator of the ventilation state of intermediate waters, since aged waters with higher CO₂ are corrosive to aragonite/calcite. It was proposed that the ventilation from southern source was cutoff leading to a continuous build-up of oxygen deficient waters in the Arabian Sea (Pichevin et al., 2007). This happened as a result of sluggish circulation of the Red Sea and Persian Gulf waters since the early Holocene, which increased progressively with rising sea level until it reached its present state at around 6 ka BP (Pichevin et al., 2007). The aragonite content from Core SK-17 shows a continuous decrease through the Holocene (Fig. 2e) along with an increase in thermocline foraminifera species *Globorotalia menardii*, which suggests decreasing thermocline ventilation through the Holocene (Singh et al., 2018). Decreasing thermocline ventilation led to build-up of corrosive waters, leading to lowered pH and a consequent decrease in the aragonite content through time. This aragonite trend is broadly consistent with the decreasing CaCO₃ content from Core BP3-GCR3. Therefore our CaCO₃ and OC values in conjunction with data from SK-17 suggests that progressively decreasing ventilation combined with increasing productivity must have led to an increase in corrosiveness of bottom waters through the Holocene.

5. Conclusions

The Mn and Fe liberated from the reduction of oxide particulates in sediments underlying intense OMZ of the EAS provide reliable proxy for paleo-redox conditions. The time-series of a set of redox-sensitive elements extracted from the dispersed oxide particulates in the sediment of the Eastern Arabian Sea indicate consistently intensified core of the OMZ through the Holocene. The intensification of OMZ seems to be a result of increased export production coupled with decreased ventilation of thermocline waters through the Holocene as supported by other studies in this region. A rapid increase in the organic carbon content and concomitant rapid decrease in CaCO₃ content at around 5.5 ka BP suggests carbonate dissolution due to increased intensity of the core of the OMZ due to intense suboxia to anoxia.

References

- Agnihotri, R., Dutta, K., Bhushan, R., Somayajulu, B.L.K. (2002) Evidence for solar forcing on the Indian monsoon during the last millennium. *Earth Planet. Sci. Lett.*, v.198, pp.521–527. doi:10.1016/S0012-821X(02)00530-7
- Agnihotri, R., Bhattacharya, S.K., Sarin, M.M., Somayajulu, B.L.K. (2003) Changes in surface productivity and subsurface denitrification during the Holocene: A multiproxy study from the eastern Arabian Sea. *Holocene.*, v.13, pp.701–713. doi:10.1191/0959683603hl656rp
- Altabet, M.A., Francois, R., Murray, D.W., Prell, W.L. (1995) Climate-related variations in denitrification in the Arabian Sea from sediment $^{15}\text{N}/^{14}\text{N}$ ratios. *Nature.*, v.373, pp.506–509. doi:10.1038/373506a0
- Banakar, V.K., Oba, T., Chodankar, A. R., Kuramoto, T., Yamamoto, M., Minagawa, M. (2005) Monsoon related changes in sea surface productivity and water column denitrification in the Eastern Arabian Sea during the last glacial cycle. *Mar. Geol.*, v.219, pp.99–108. doi:10.1016/j.margeo.2005.05.004
- Banakar, V. K., Hein, J. R., Rajani, R. P., Chodankar, A. R. (2007) Platinum group elements and gold in ferromanganese crusts from Afanasiy-Nikitin seamount, equatorial Indian Ocean: Sources and fractionation. *J. Earth Syst. Sci.*, v.116, pp.3–13. doi:10.1007/s12040-007-0002-x
- Banakar, V.K. (2010) Deep-sea ferromanganese deposits and their resource potential for India. *J Indian Inst. Sci.*, v.90, :535–541.
- Banse, K. (1968) Hydrography of the Arabian Sea Shelf of India and Pakistan and effects on demersal fishes. *Deep Res. Oceanogr. Abstr.*, v.15, pp.45–79. doi:10.1016/0011-7471(68)90028-4
- Bayon, G., German, C.R., Boella, R.M., Milton, J.A., Taylor, R.N., Nesbitt, R.W., (2002) An improved method for extracting marine sediment fractions and its application to Sr and Nd isotopic analysis. *Chemical Geology.*, v.187, pp.179–199. doi:10.1016/S0009-2541(01)00416-8
- Bhattathiri, P.M.A., Pant, A., Sawant, S., Gauns, M., Matondkar, S.G.P., and Mohanraju, R. (1996) Phytoplankton production and chlorophyll distribution in the eastern and central Arabian Sea in 1994-1995. *Curr Sci.*, v.79, pp. 857–862.
- Bhushan, R., Dutta, K., Somayajulu, B.L.K., (2001) Concentrations and burial fluxes of organic and inorganic carbon on the eastern margins of the Arabian Sea. *Mar. Geol.*, v.178, pp.95–113. doi:10.1016/S0025-3227(01)00179-7
- Cabarcos. E., Flores, J.A., Singh, A.D., Sierro, F.J., (2014) Monsoonal dynamics and evolution of the primary productivity in the eastern Arabian Sea over the past 30 ka. *Palaeogeogr. Palaeoclimatol. Palaeoecol.*, v.411, pp.249–256. doi:10.1016/j.palaeo.2014.07.006
- Calvert, S.E., Pedersen, T.F. (1996) Sedimentary geochemistry of manganese: Implications for the environment of formation of manganiferous black shales. *Econ. Geol.*, v.91, pp.36–47. doi:10.2113/gsecongeo.91.1.36

- Das, M., Singh, R.K., Gupta, A.K., Bhaumik, A.K., (2017) Holocene strengthening of the Oxygen Minimum Zone in the northwestern Arabian Sea linked to changes in intermediate water circulation or Indian monsoon intensity? *Palaeogeogr. Palaeoclimatol. Palaeoecol.*, v.483, pp.125–135. doi:10.1016/j.palaeo.2016.10.035
- Dickens, G.R., Owen, R.M., (1994) Late Miocene-Early Pliocene manganese redirection in the central Indian Ocean: Expansion of the Intermediate Water oxygen minimum zone. *Paleoceanography.*, v.9, pp.169–181. doi:10.1029/93PA02699
- Frank, M., O’Nions, R.K., Hein, J.R., Banakar, V.K., (1999) 60 Myr records of major elements and Pb-Nd isotopes from hydrogenous ferromanganese crusts: Reconstruction of seawater paleochemistry. *Geochim. Cosmochim. Acta.*, v.63, pp.1689–1708. doi:10.1016/S0016-7037(99)00079-4
- Gaye, B., Böll, A., Segschneider, J., Burdanowitz, N., Emeis, K.C., Ramaswamy, V., Lahajnar, N., Lückge, A., Rixen, T. (2018) Glacial-interglacial changes and Holocene variations in Arabian Sea denitrification. *Biogeosciences.*, v.15, pp.507–527. doi:10.5194/bg-15-507-2018
- GEBCO compilation group. (2020) GEBCO Gridded Bathymetry Data. In: 2020. https://www.gebco.net/data_and_products/gridded_bathymetry_data/. Accessed 5 Jun 2020
- German, C.R., Elderfield, H. (1990) Application of the Ce anomaly as a paleoredox indicator: the ground rules. *Paleoceanography.*, v.5, pp.823–833. doi:10.1029/PA005i005p00823
- Glasby, G.P., Mountain, B., Vineesh, T.C., Banakar, V.K., Rajani, R., Ren, X. (2010) Role of hydrology in the formation of Co-rich Mn crusts from the equatorial N pacific, equatorial S Indian ocean and the NE Atlantic ocean. *Resour. Geol.*, v.60, pp.165–177. doi:10.1111/j.1751-3928.2010.00123.x
- Godad, S.P., Naik, S.S., Naidu, P.D., (2017) 70 kyr record of denitrification and oxygenation changes in the eastern Arabian Sea. *Geochem. J.*, v.51, pp.329–336. doi:10.2343/geochemj.2.0472
- Grill, E. V., (1982) Kinetic and thermodynamic factors controlling manganese concentrations in oceanic waters. *Geochim. Cosmochim. Acta.*, v.46, pp.2435–2446. doi:10.1016/0016-7037(82)90366-0
- Gupta, A.K., Singh, R.K., Joseph, S., Thomas, E. (2004) Indian Ocean high-productivity event (10–8Ma): linked to global cooling or to the initiation of the Indian monsoons. *Geology.*, v.32, pp.753–756 doi:10.1130/G20662.1
- Joseph, S., Freeland, H.J. (2005) Salinity variability in the Arabian Sea. *Geophys. Res. Lett.*, v.32 pp.1–4. doi:10.1029/2005GL022972
- Kessarkar, P.M., Naqvi, S.W.A., Thamban, M., Fernandes, L.L., Siebert, C., Rao, V.P., Kawahata, H., Ittekkot, V., Frank, M. (2018) Variations in Denitrification and Ventilation Within the Arabian Sea Oxygen Minimum Zone During the Holocene. *Geochem. Geophys. Geosys.* v.19, pp.2179–2193. doi:10.1029/2017GC007286
- Lachkar, Z., Smith, S., Lévy M., Pauluis, O. (2016) Eddies reduce denitrification and compress habitats in the Arabian Sea. *Geophys. Res. Lett.* v.43, pp.9148–9156. doi:10.1002/2016GL069876

- Lawler, A. (2008) Boring No More, a trade-savvy Indus Emerges. *Science*. v.320 (5881), pp.1267–1281. doi: 10.1126/science.320.5881.1276
- Lewis, B.L., Luther, G.W. (2000) Processes controlling the distribution and cycling of manganese in the oxygen minimum zone of the Arabian Sea. *Deep. Res. Part II, Top. Stud. Oceanogr.*, v.47, pp.1541–1561. doi:10.1016/S0967-0645(99)00153-8
- Madhupratap, M., Kumar, S.P., Bhattathiri, P. M. A., Kumar, M.D., Raghukumar, S., Nair, K.K.C., Ramaiah, N. (1996) Mechanism of the biological response to winter cooling in the northeastern Arabian Sea. *Nature*., v.384 (6609) pp.549–52. doi:10.1038/384549a0
- Martin, J.H., Knauer, G.A. (1984) VERTEX: Manganese transport through oxygen minima. *Earth Planet Sci. Lett.* v.67, pp.35–47. doi:10.1016/0012-821X(84)90036-0
- McCreary, J.P., Yu, Z., Hood, R.R., Vinayachandran, P.N., Furue, R., Ishida, A., Richards, K.J. (2013) Dynamics of the Indian-Ocean oxygen minimum zones. *Prog. Oceanogr.*, v.112–113, pp.15–37. doi:10.1016/j.pocean.2013.03.002
- Morrison, J.M., Codispoti, L.A., Smith, S.L., Wishner, K., Flagg, C., Gardner, W.D., Gaurin, S., Naqvi, S.W.A., Manghnani, V., Prosperie, L., Gundersen, S.J. (1999) The oxygen minimum zone in the Arabian Sea during 1995. *Deep. Res. Part II, Top. Stud. Oceanogr.*, v.46, pp.1903–1931. doi:10.1016/S0967-0645(99)00048-X
- Nagoji, S.S., Tiwari, M. (2017) Organic carbon preservation in Southeastern Arabian Seasediments since mid-Holocene: Implications to South Asian Summer Monsoon variability. *Geochem. Geophys. Geosys.*, v.116, pp.1–12. doi:10.2113/2.4.476
- Naidu, P.D., Singh, A.D., Ganeshram, R., Bharti, S.K. (2014) Abrupt climate-induced changes in carbonate burial in the Arabian Sea: Causes and consequences *Geochem. Geophys. Geosyst.* v.15(1) pp.1398–1406. doi:10.1002/2013GC005065
- Naik, S.S., Godad, S.P., Naidu, P.D., Tiwari, M., Paropkari, A. L. (2014) Early- to late-Holocene contrast in productivity, OMZ intensity and calcite dissolution in the eastern Arabian Sea. *Holocene*., v.24(6), pp.749–755. doi:10.1177/0959683614526936
- Naik, S.S., Naidu, P.D., Foster, G.L., Martínez-Botí, M.A. (2015) Tracing the strength of the southwest monsoon using boron isotopes in the eastern Arabian Sea *Geophys. Res. Lett.* v.42, pp.1450–1458. doi:10.1002/2015GL063089.
- Naqvi, S.W.A. (1991) Geographical extent of denitrification in the Arabian Sea in relation to some physical processes. *Oceanologica. Acta.*, v.14, pp.281–290.
- Narayana, A.C., Naidu, P.D., Shinu, N., Nagabhushanam, P., Sukjija, B.S. (2009), Carbonate and organic carbon content changes over last 20 ka in the Southeastern Arabian Sea: Paleoceanographic implications, *Quat. Int.*, v.206, pp.72– 77, doi:10.1016/j.quaint.2008.10.010
- Olson, D.B., Hitchcock, G.L., Fine, R.A., Warren, B.A. (1993) Maintenance of the low-oxygen layer in the central Arabian Sea. *Deep. Res. Part II.*, v.40, pp.673–685. doi:10.1016/0967-0645(93)90051-N

- Pattan, J.N., Pearce, N.J.G., Mislankar, P.G. (2005) Constraints in using Cerium-anomaly of bulk sediments as an indicator of paleo bottom water redox environment: A case study from the Central Indian Ocean Basin. *Chem. Geol.*, v.221, pp.260–278. doi:10.1016/j.chemgeo.2005.06.009
- Pattan, J.N., Parthiban, G., Garg, A., Moraes, N.R.C. (2017) Intense reducing conditions during the last deglaciation and Heinrich events (H1, H2, H3) in sediments from the oxygen minimum zone off Goa, eastern Arabian Sea. *Mar. Pet. Geol.*, v.84, pp.243–256. doi:10.1016/j.marpetgeo.2017.03.034
- Picchevin, L., Bard, E., Martinez, P., Billy, I. (2007) Evidence of ventilation changes in the Arabian Sea during the late Quaternary: Implication for denitrification and nitrous oxide emission. *Global Biogeochem. Cycles.*, v.21, pp.1–12. doi:10.1029/2006GB002852
- Prasad, V., Farooqui, A., Sharma, A., Phartiyal, B., Chakraborty, S., Bhandari, S., Raj. R., Singh, A. (2014) Mid-late Holocene monsoonal variations from mainland Gujarat, India: A multi-proxy study for evaluating climate culture relationship. *Palaeogeogr. Palaeoclimatol. Palaeoecol.* v.397, pp.38–51. doi:/10.1016/j.palaeo.2013.05.025
- Kumar, S.P., Madhupratap, M., Kumar, M.D., Muraleedharan, P.M. De Souza, S.N., Gauns, M., Sarma, V.V.S.S. (2000) Physical control of primary productivity on a seasonal scale in central and eastern Arabian Sea. *Proc. Indian. Acad. Sci. (Earth Planet. Sci.)* v.109, pp.433–441. doi: 10.1007/bf02708331
- Qasim, S. (1977) Biological productivity of the Indian Ocean. *Indian. J. Geo-Marine. Sci.*, v.06, pp.122–137.
- Raikes, R.L. (1964) The End of the Ancient Cities of the Indus Robert. *Am. Anthropol. Assoc.*, v.66, pp.284–299. doi:10.1017/CBO9781107415324.004
- Raj, R., Chamyal, L.S., Prasad, V., Sharma, A., Tripathi, J.K., Verma, P. (2015) Holocene climatic fluctuations in the Gujarat Alluvial Plains based on a multiproxy study of the Pariyaj Lake archive, western India. *Palaeogeogr. Palaeoclimatol. Palaeoecol.* v.421, pp.60–74. doi:10.1016/j.palaeo.2015.01.004
- Rajani, R.P., Banakar, V.K., Parthiban, G., Mudholkar, A.V., Chodankar, A.R. (2005) Compositional variation and genesis of ferromanganese crusts of the Afanasiy-Nikitin Seamount, Equatorial Indian Ocean. *J. Earth Syst.Sci.*, v.114, pp.51–61. doi:10.1007/BF02702008
- Resplandy, L., Lévy, M., Bopp, L., Echevin, V., Pous, S., Sarma, V.V.S.S., Kumar, M.D.(2012) Controlling factors of the oxygen balance in the Arabian Sea's OMZ. *Biogeosciences.*, v.9, pp.5095–5109. doi:10.5194/bg-9-5095-2012
- Rutberg, R.L., Hemming, S.R., Goldstein, S.L. (2000) Reduced North Atlantic Deep Water flux to the glacial Southern Ocean inferred from neodymium isotope ratios. *Nature.*, v.405, pp.935–938. doi:10.1038/35016049
- Saager, P.M. (1994) The biogeochemical distribution of trace elements in the Indian Ocean. *Proc. Indian. Acad. Sci.(Earth Planet. Sci)* v.103, pp.237–278. doi:10.1007/BF02839538
- Saager, P.M., De Baar H.J.W., Burkill, P.H. (1989) Manganese and iron in Indian Ocean waters. *Geochim. Cosmochim. Acta.* v.53, pp.2259–2267. doi:10.1016/0016-7037(89)90348-7

- Schenau, S. J., Reichart, G. J., De Lange, G.J. (2002) Oxygen minimum zone controlled Mn redistribution in Arabian Sea sediments during the late Quaternary. *Paleoceanography.*, v.17,pp.3–4. doi:10.1029/2000
- Singh, A.D., Kroon, D., Ganeshram, R.S. (2006) Millennial scale variations in productivity and OMZ intensity in the eastern Arabian Sea. *J. Geol. Soc. India.*, v.68, pp369–377.
- Singh, A.D. (2007) Episodic preservation of pteropods in the eastern Arabian Sea: Monsoonal change, oxygen minimum zone intensity and aragonite compensation depth. *Indian. J. Mar. Sci.*, v.36, pp.378–383
- Singh, A.D., Jung, S.J.A., Darling, K., Ganeshram, R. S., Ivanochko, T., Kroon, D. (2011) Productivity collapses in the Arabian Sea during glacial cold phases. *Paleoceanography.*, v.26, pp.1–10. doi:10.1029/2009PA001923
- Singh, A.D., Rai, A.K., Verma, K., Das, S., Bharti, S.K. (2015) Benthic foraminiferal diversity response to the climate induced changes in the eastern Arabian Sea oxygen minimum zone during the last 30 ka BP. *Quat. Int.*, v.374, pp.118–125. doi:10.1016/j.quaint.2014.11.052
- Singh, A.D., Jung, S.J.A., Anand, P., Kroon, D., Ganeshram, R.S. (2018) Rapid switch in monsoon-wind induced surface hydrographic conditions of the eastern Arabian Sea during the last deglaciation. *Quat. Int.* v.479, pp.3–11. doi:10.1016/j.quaint.2018.03.027
- Somayajulu, B.L.K., Yadav, D.N., Sarin, M.M. (1994) Recent sedimentary records from the Arabian Sea. *Proc. Indian. Acad. Sci. (Earth Planet. Sci.)* v.103, pp.315–327. doi:10.1007/BF02839541
- Southon, J., Kashgarian, M., Fontugne, M., Metivier, B., Yim, W.W.S. (2002) Marine reservoir corrections for the Indian Ocean and Southeast Asia. *Radiocarbon.*, v.44 pp.167–180. doi:10.1017/S0033822200064778
- Sruthi, K. V., Kurian, P.J., Rajani, P.R. (2014) Distribution of major and trace elements of a sediment core from the eastern Arabian Sea and its environmental significance. *Curr Sci.* v.107,pp. 1161–1167.
- Staubwasser, M., Sirocko, F., Grootes, P.M., Segl, M. (2003) Climate change at the 4.2 ka BP termination of the Indus valley civilization and Holocene south Asian monsoon variability. *Geophys Res. Lett.* v.30, pp.3–6. doi:10.1029/2002GL016822
- Stuiver, M., Reimer, P.J. (1993) Extended 14C data base and revised CALIB 3.0 14C age calibration program. *Radiocarbon.* v.35, pp.215–230.
- Tamura, H., Goto, K., Nagayama, M. (1976) The effect of ferric hydroxide on the oxygenation of ferrous ions in neutral solutions. *Corros. Sci.*, v.16, pp.197–207. doi:10.1016/0010-938X(76)90046-9
- Taylor, S.R., McLennan, S.M. (1985) *The Continental Crust: its Composition and Evolution. An Examination of the Geochemical Record Preserved in Sedimentary Rocks.* Blackwell, Oxford 312.
- Turekian, K.K., Wedepohl, K.H. (1961) Distribution of the Elements in Some Major Units of the Earth's Crust. *Geol Soc. Am. Bull.* v.72,pp.175–192.

Verma, K., Bharti, S.K., Singh, A.D. (2018) Late Glacial–Holocene record of benthic foraminiferal morphogroups from the eastern Arabian Sea OMZ: Paleoenvironmental implications. *J. Earth Syst. Sci.*, v.127, pp.21–36. doi:10.1007/s12040-018-0920-9

Weijden, CH. Van. Der., Reichart, G. J., Os, B.J.H. Van. (2006) Sedimentary Trace Element Records over the last 200 Kyr from within and below the Northern Arabian Sea Oxygen Minimum Zone. *Mar Geol.*, v.231, pp.69–88. doi:10.1016/j.margeo.2006.05.013

Wyrtki, K. (1973) Physical Oceanography of the Indian Ocean. pp.18–36. doi:10.1007/978-3-642-65468-8_3

You, Y. (1997) Seasonal variations of thermocline circulation and ventilation in the Indian Ocean. *J. Geophys Res. Ocean.*, v.102, pp.10391–10422. doi:10.1029/96JC03600

Figure Legends

Figure 1. Location of sediment core BP3GCR3 shown on bathymetric map of the Arabian Sea shown with a filled diamond. Core SK-17 (Singh et al., 2006) in proximity to our core and used for comparison, is marked with a filled black circle. The depth profiles of dissolved oxygen (μmol) and dissolved Mn (nmol) in the water column at 19°N ; 67°E (station 6, Saager et al., 1989) are shown as inset. These profiles are assumed to be valid for the BP3GCR3 location. (Source of bathymetric map: GEBCO compilation group 2020)

Figure 2. Time-series of a) oxide -Mn and -Fe from BP3GCR3, b) oxide -Co and -Ce contents in BP3GCR3, c) High O_2 taxa from SK-17 (Singh et al., 2015), d) organic carbon (OC) and CaCO_3 in BP3GCR3 and e) Aragonite % and *G. bulloides*/*G. ruber* ratio (Singh et al., 2011), for the last 10.5 kyr. Vertical dotted line at 5.5 ky BP marks a distinct change in distribution of oxide-Mn and -Fe contents from above their respective Holocene-mean to below mean values (broken horizontal lines with corresponding colour codes). A rapid downward shift from $\sim 10\%$ to $\sim 2\%$ in OC and contrasting upward shift from $\sim 30\%$ to $\sim 55\%$ are distinctly expressed. Downward arrows on horizontal axis are the radiocarbon ages.

Figure 3. Depth-age curve for BP3GCR3 showing sedimentation rates (cm/ky) between two adjacent radiocarbon dated sections.

Figure 4. X-Y scatter plots of organic carbon (OC) versus CaCO_3 exhibiting two contrasting mutual relationships for $> 2\%$ and $< 2\%$ of OC.

Table Legends

Table 1 Radiocarbon ages of BP3GCR3 sediment core.

Table 2 Recovery efficiency of leaching method assessed by analysing leachates of three international reference manganese nodules which are genetically similar to sedimentary dispersed oxide Mn particulates.

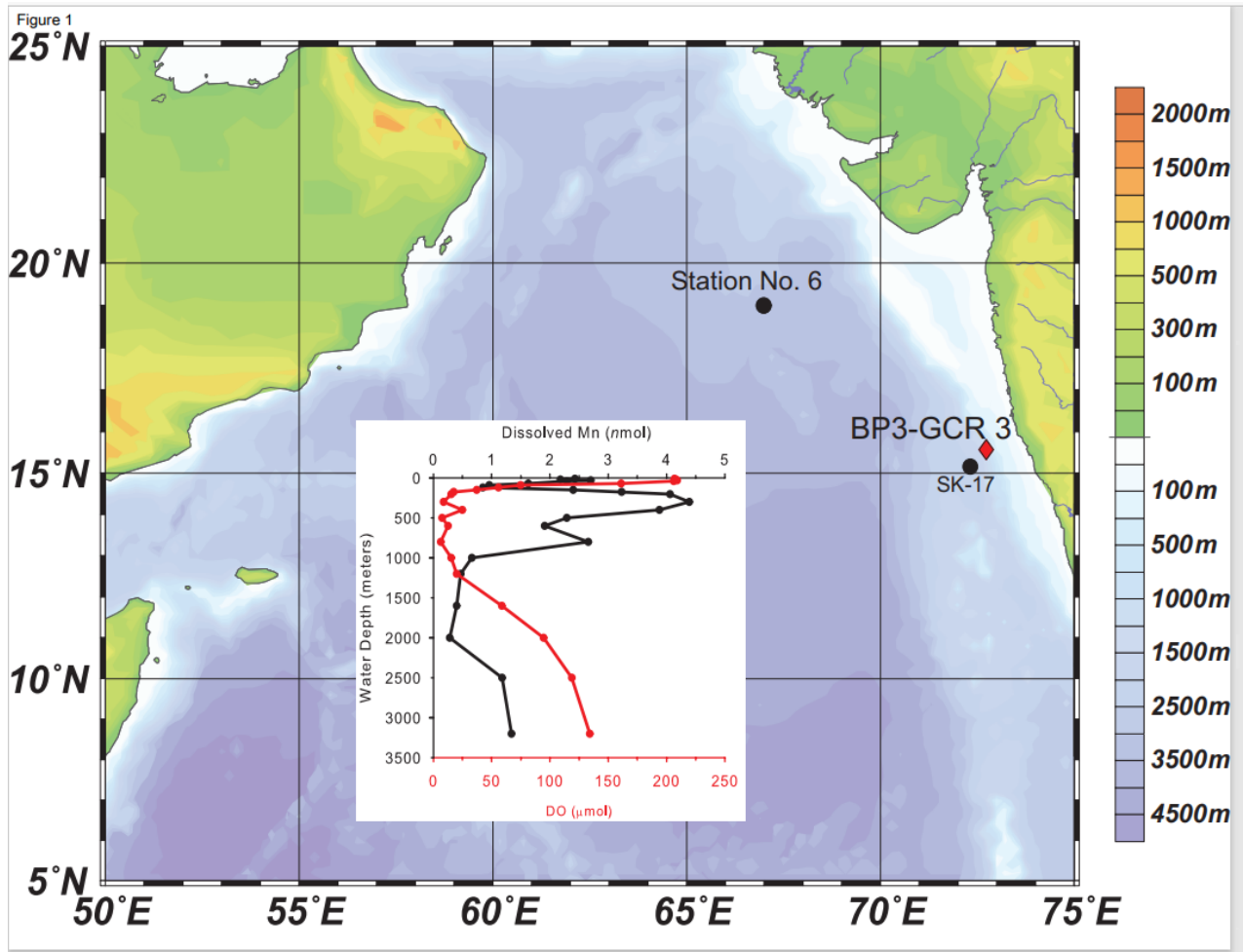


Fig. 1

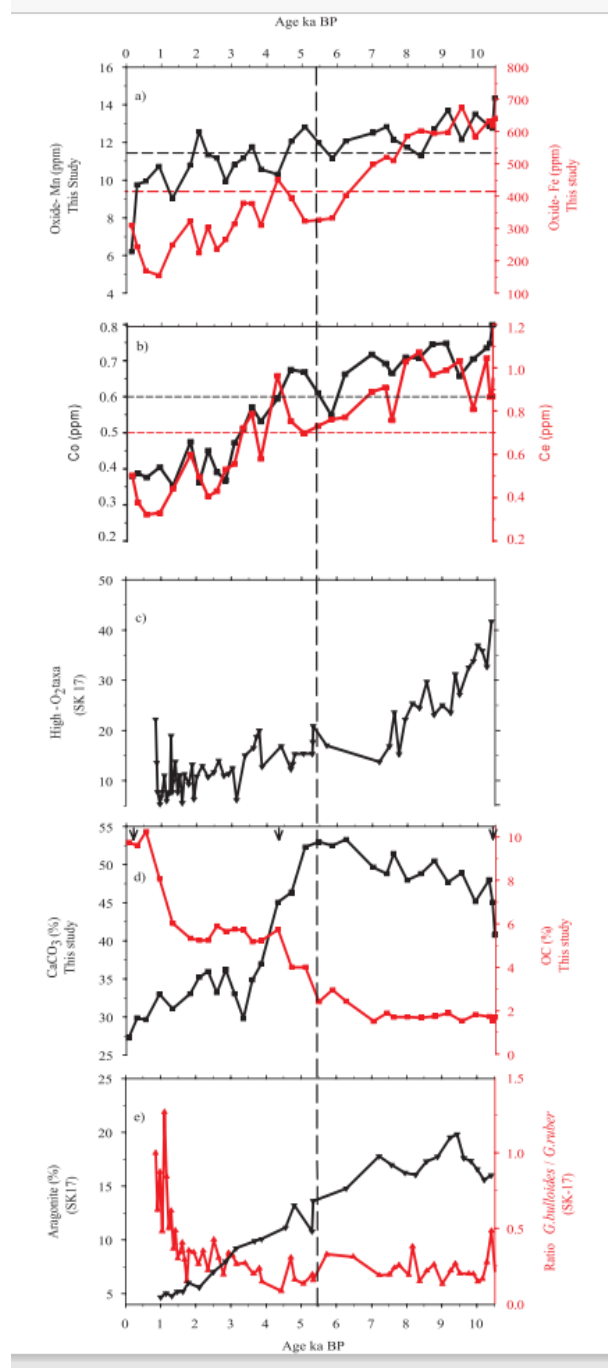


Fig. 2

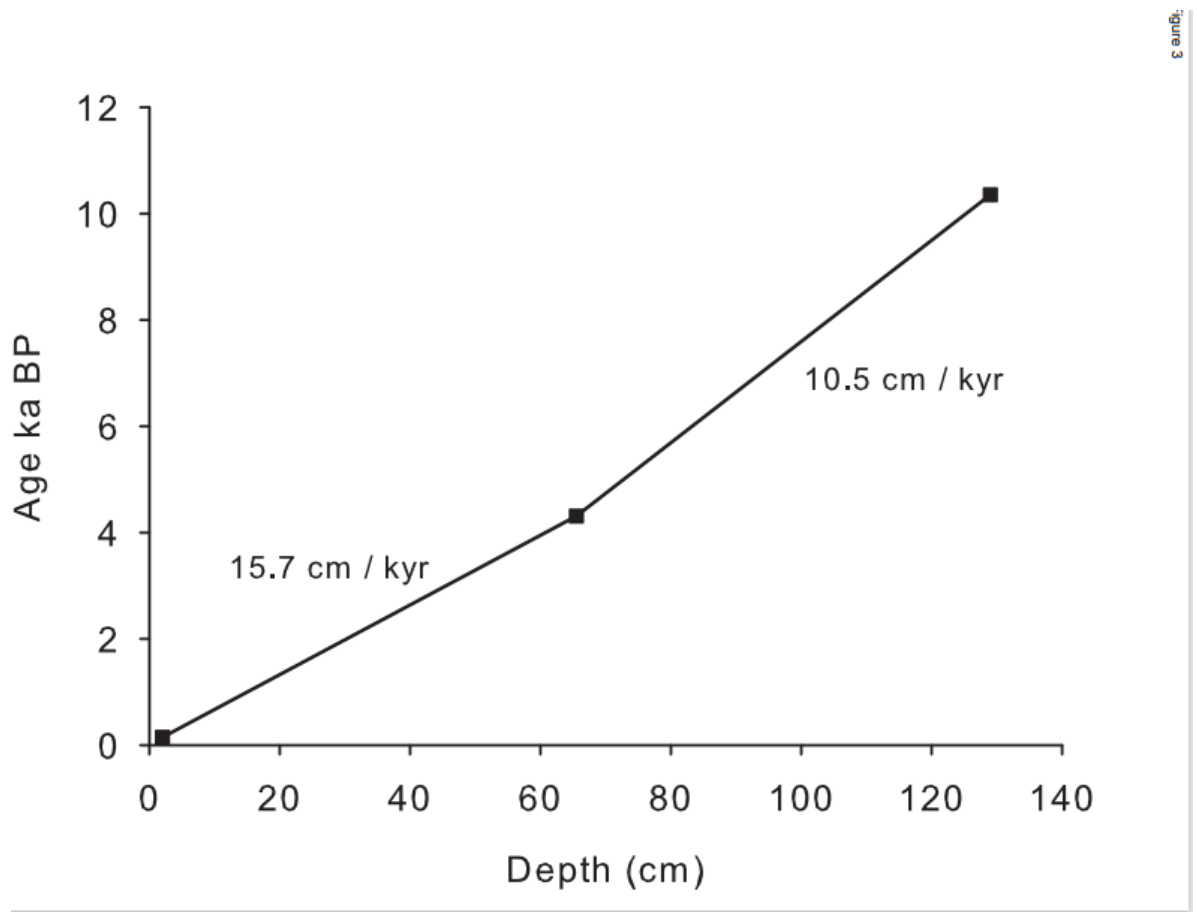


Fig. 3

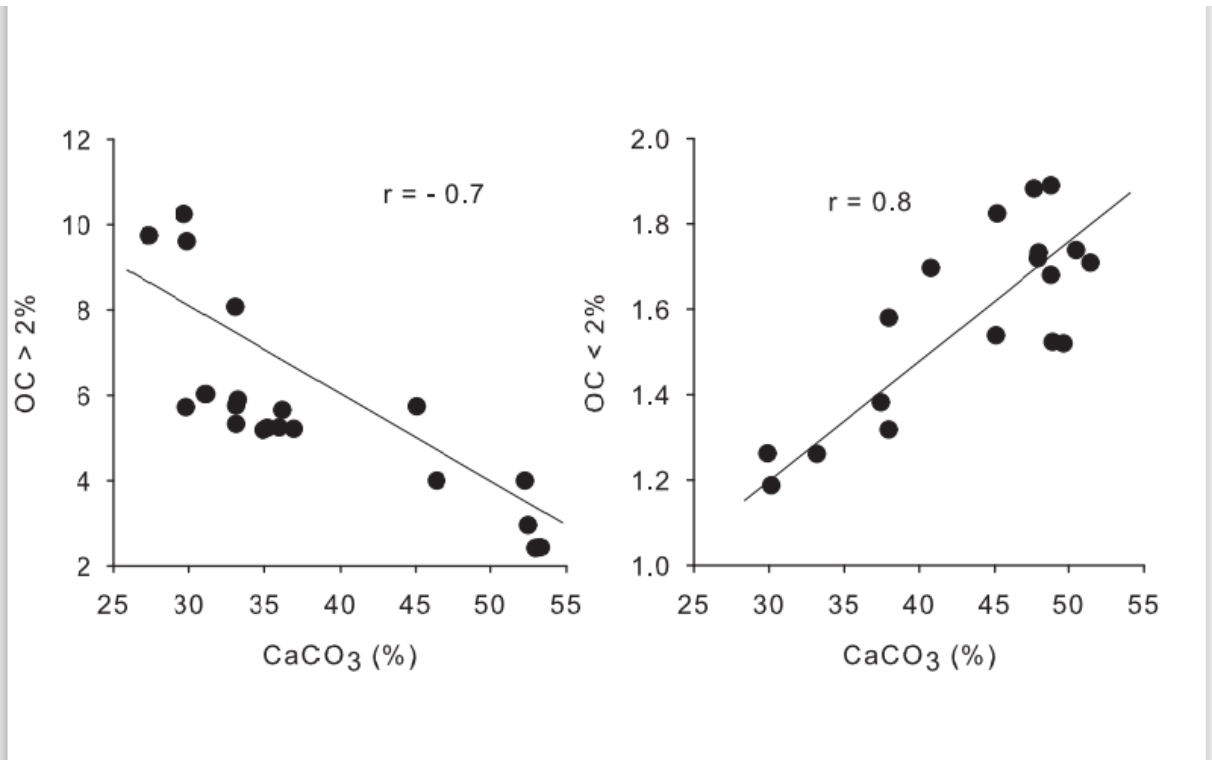


Fig. 4

Table 1.

Depth (cm)	¹⁴ C Age (yr BP)	Error ± yrs	RC Age (yr BP)*	Cal Age (y BP)**
2	696	35	74	149±118
65.5	4304	37	3682	4311±55
129	9673	44	9051	10356±19

*Reservoir age corrected ¹⁴C dates considering a reservoir age of 622 y for the Eastern Arabian Sea region (Southon et al. 2002) **Calendar ages calibrated using CALIB7.1 radiocarbon age calibration with 1950 AD as reference year (Stuiver and Reimer 1993); <http://www.calib.org>.

Table 2

Reference Standard*							BP3GCR3 (elements in ppm)		
JMn-1		USGS-A1		USGS-P1					
Element	Certified	Analyzed	Certified	Analyzed	Certified	Analyzed	Min	Max	Average
Fe (%)	10.1	9.7	10.9	10.1	5.8	5.4	155	683	422
Mn (%)	25.6	25.3	18.5	19.8	29.1	29.0	6.2	14.4	11.6

* - JMn1 = Japanese manganese nodule; USGS A1 - Atlantic manganese nodule; USGS P1 - Pacific manganese nodule.